http://dx.doi.org/10.1016/j.ijmecsci.2018.07.027

Influence of size effect and plastic strain gradient on the springback behavior of metallic materials in microbending process

J.L. Wang[a], M.W. Fu[a, b *], S.Q. Shi[a], A. M. Korsunsky[c]

[a] Department of Mechanical Engineering, The Hong Kong Polytechnic University, Hung Hom, Kowloon, Hong Kong

[b] PolyU Shenzhen Research Institute, No. 18 Yuexing Road, Nanshan District, Shenzhen, PR China

[c] Multi-Beam Laboratory for Engineering Microscopy (MBLEM), Department of Engineering Science, University of Oxford, Parks Rd, Oxford OX1 3PJ, U.K.

*Tel: 852-27665527, Email: mmmwfu@polyu.edu.hk

Abstract

In micro-bending process, the size effect induced by the variation of grain size and geometrical size (the thickness) of sheet metals, represented by the ratio of surface grain number to the total grain number of workpiece (η), and strain gradient effect are the key factors affecting the bending behaviour and springback angle. The interaction of the grain-based size effect and the strain gradient effect on springback has not yet been fully understood and investigated in micro-scaled bending of metallic materials. In this research, a combined constitutive model simultaneously considering both the grain size effect and strain gradient was proposed. The theoretical calculation was conducted using the proposed model, and quantitative evaluation was made of the contribution from each kind of size effect on the springback angle. The springback angle due to strain gradient size effect decreases with the increase of sheet thickness and the decrease of the grain size. Pure microbending experiments using copper alloy sheet metal samples with the thickness of 0.1, 0.2, and 0.4 mm were conducted, and the springback angles calculated using the established model were corroborated by the experimental results, providing model validation. The reported results thus provide an in-depth understanding of the grain-geometrical size effect and strain gradient size effect influence on the springback behaviour in micro-bending of metallic materials.

Keywords: Size effect, Strain gradient, Microbending, Springback

1. Introduction

In the past several decades, the rapid development of micro-medical systems, MEMS (micro electro mechanical systems) and advances in the micro-electronics industry has led to a tremendous increase in the demand for micro-scaled parts, such as micro-leaf springs, micro-pogo pins, etc. Micro-scale sheet metal forming has thus become an important manufacturing processes for the production of microparts (Engel and Eckstein, 2002; Fu et al., 2016; Fu and Chan, 2013; Geiger et al., 2001; Vollertsen et al., 2006). In the micro-bending process, the springback observed upon the removal of external loading is controlled by the material elasto-plastic deformation characteristics, and has a profound effect on the dimensional accuracy and geometric precision of micro-bent parts (Wagoner et al., 2013). To ensure reliable high quality of the micro-parts, it is essential to study and understand the springback behavior in microforming processes, and its correlation with the dimensional accuracy and geometric precision of micro-bent parts.

Size effects in the micro-bending process is induced by the relative variation of grain size and geometric dimension (sheet thickness), represented as the ratio of the number of surface grains to the overall grain number (η) in the workpiece, and the strain gradient effect that can be quantified by the ratio of the sample thickness to the radius of bending curvature. These key factors affect the bending behaviour and springback angle (Diehl et al., 2008; Fleck and Hutchinson, 1993, 2001; Li et al., 2010; Liu et al., 2011; Wang et al., 2014). In terms of grain and geometrical size effects, three-point bending (Liu et al., 2011), micro U-bending (Wang et al., 2014), and L-bending (Diehl et al., 2010) experiments were conducted using copper sheet to study the influence of grain and geometrical size effects on springback. It was found that generally the springback angle tends to decrease with the increase of the sheet thickness. It is also found that the springback angle does not vary monotonously with η. Furthermore,

due to the crystal anisotropy of the surface grain, the scatter of the experimental result becomes obviously with the increasing η. Diehl et al. (Diehl et al., 2010) found that the scatter of the springback angle is significantly increased with η. In the study of grain and geometrical size effects in microforming processes, the surface layer model (Geiger et al., 2001; Ran et al., 2013; Xu et al., 2015), the composite model (Meyers and Ashworth, 1982), and the crystal plasticity based model (Ran and Fu, 2014; Wang et al., 2009; Zhuang and Lin, 2008; Zhuang et al., 2010) were proposed to describe and represent the influence of the size effects on the deformation behaviour of materials.

Strain gradient effect, on the other hand, exerts an opposite influence on the springback angle compared to the grain and geometrical size effects. It is found that the springback angle decreases with the sheet thickness when the sheet thickness is smaller than about 0.1mm (Diehl et al., 2010). Fleck and Hutchinson (Fleck and Hutchinson, 1993, 2001) formulated the phenomenological strain gradient plasticity theory which considers the hardening effect induced by strain gradient in micro-scale bending process. Subsequently, the relationship between the non-dimensional bending curvature and the non-dimensional bending moment for metallic plates with the thickness from a few mm down to about 10 nm was developed (Zhu and Karihaloo, 2008). The strain gradient effect was found to play an important role in the effective bending strength at the micro-scale (Wang et al., 2003). A work hardening law due to both the statistically stored dislocations (SSD) and geometrically necessary dislocations (GND) was developed, with the latter being directly related to the plastic strain gradient (Nix and Gao, 1998; Zbib and Aifantis, 2003). Li et al. (Li et al., 2010) proposed a constitutive model considering the plastic strain and plastic strain gradient hardening based on the yield stress and dislocation density to predict the springback angle due to microbending by analytical calculation.

From the abovementioned research, it can be deduced that the springback is mainly affected by either grain and geometrical size effect, or the strain gradient size effect. However, the interaction and competition between the grain-geometrical size effect and the strain gradient size effect on springback have not yet been investigated extensively in micro-scale bending processes. Therefore, in order to explain accurately the underlying mechanism of springback, an appropriate constitutive model is required that considers simultaneously both the geometric and strain gradient size effects. This is the objective is the present study. The constitutive model based on the traditional surface layer model is used to explain the grain-geometric size effect, while the strain gradient is taken into account via embedding the higher order of strain into the model. To corroborate the results using the proposed constitutive model, a tooling set was designed to perform pure bending behaviour of copper alloy sheet with the thickness of 0.1, 0.2, and 0.4 mm. The theoretical calculation of the springback was conducted, and the model was validated. The experimental results thus provide a validated in-depth understanding of springback behaviour affected by the microstructural and geometrical size effect, and simultaneously the influence of strain gradient effects, in such a way as to control more efficiently the precision of fabricated sample geometry and shape, and further dimensional accuracy of microbent sheet metal parts.

2. Micro-scale U-bending experiments

2.1. Material preparation

Copper alloys are widely used in electrical and electronics industries due to their excellent electrical conductivity, excellent mechanical properties, and outstanding plastic formability. In this research, brass C2680 in sheet form was used to assess the geometric and strain gradient size effects in micro-bending. Young's modulus of the alloy is E=70-100 GPa,

Poisson's ratio ν =0.36, the shear modulus G varies from 25 to 36 GPa, and Burgers' vector for FCC crystals b= 2.608Å (2.608×10^{-10} m). Three kinds of sheet metal specimens were studied, with the thickness of 0.1mm, 0.2mm, and 0.4 mm, respectively. To eliminate the effect of rolling texture and explore the influence of grain size, the metal sheet samples with different grain sizes were obtained via annealing treatment. The annealing conditions and the obtained grain size are presented in Table 1. After the annealing heat treatment, the microstructures within the plane of the sample are shown in **Fig. 1**. The average grain size increased with the annealing temperature and holding time.

Table 1. Heat treatment parameters and the corresponding grain sizes

Annealing conditions	Case 1			Case 2			Case 3			Case 4		
	No annealing			500°C, 1h			600 °C, 2h			750 °C, 3h		
Thickness (mm)	0.1	0.2	0.4	0.1	0.2	0.4	0.1	0.2	0.4	0.1	0.2	0.4
Grain size (μm)	20	17	10.5	33	25	33	60	66	86	70	160	160
t/d	5	11.8	38	3	8	12.1	1.7	3	4.7	1.4	1.25	2.5

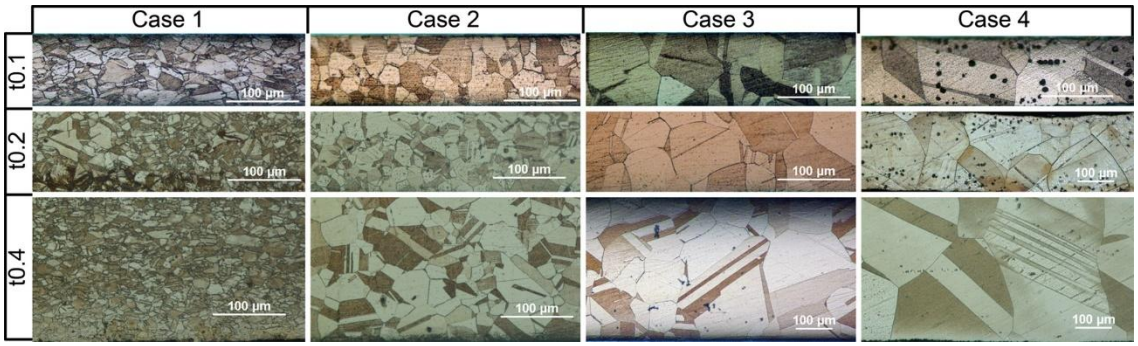

Fig. 1. Microstructures of the copper alloy across the thickness direction.

2.2. Tensile test

The mechanical properties of the copper alloy sheet were determined by the tensile test conducted in a MTS testing machine. For each type of metal sheet, three tests were conducted. The test specimen illustrated in **Fig. 2** was designed in accordance with ASTM-E8 standard.

A standard extensometer with the gauge length of 25 mm was used to measure the sample strain. The crosshead velocity is 0.033 mm/s was used in all tests. The true stress–strain curves for the four kinds of copper alloy sheet with different grain size and thickness were obtained, as shown in **Fig. 3**.

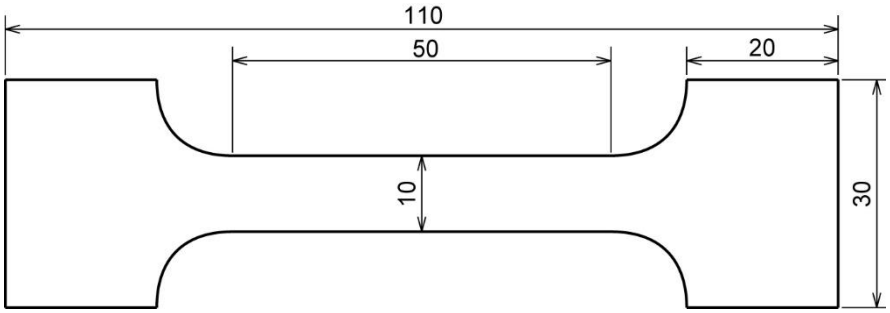

Fig. 2. Tensile test specimen.

It is found that the flow stress decreases with the increase of grain size for the sheet metal samples of the same thickness. The flow stress of the materials with different grain sizes varies significantly, in a ways that is consistent with the Hall–Petch equation (Hall, 1951; Petch, 1953). The stress–strain curves have good repeatability and consistency for the three different sheet metal samples.

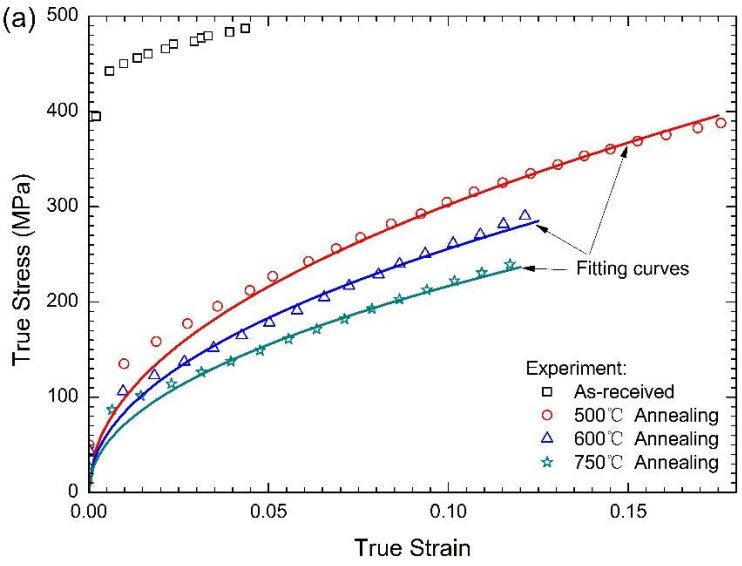

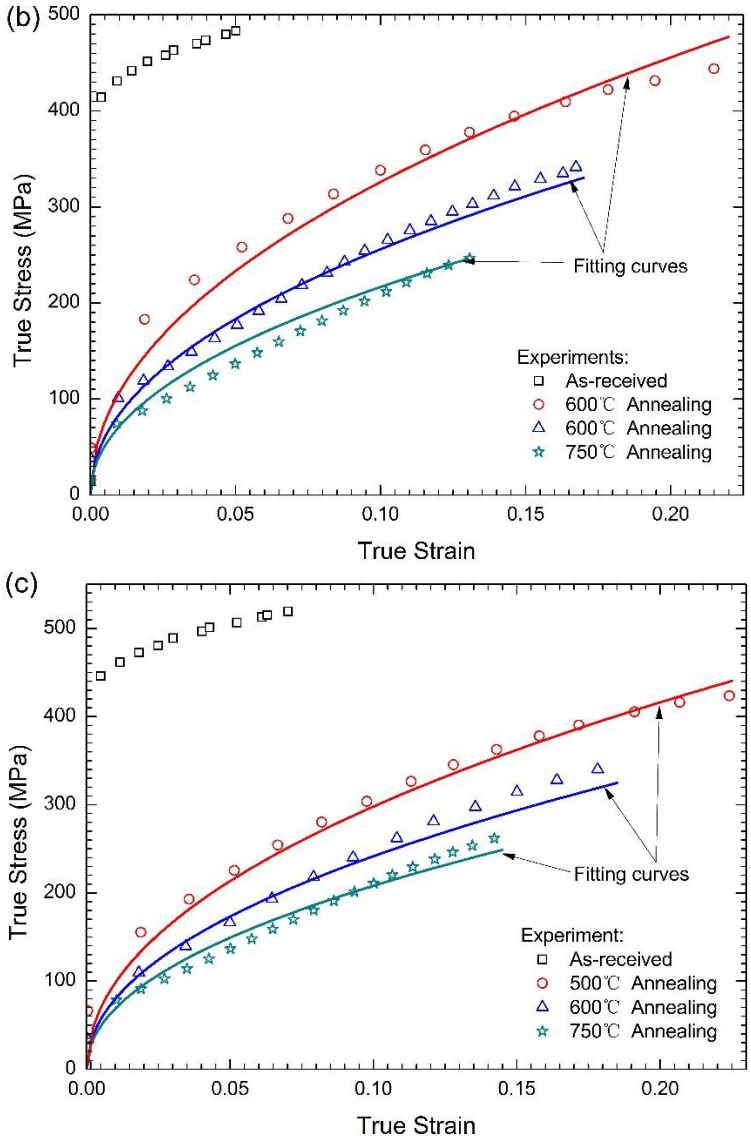

Fig. 3. True stress–strain curves of the sheet with the thickness of (a) 0.1, (b) 0.2, and (c) 0.4 mm.

2.3. Micro-scale U-bending experiments

To explore the response of samples to pure bending deformation, free U-bending tooling was designed, as shown in **Fig. 4**. Punch and die in the form of long cylinders which can freely rotate were used to reduce the effect of friction between cylinders and specimen by using lubricant such as machine oil. The radius of pressing bar (cylinders) (r) is 1.25 mm as shown in **Fig.4**. The length (le) and width (w) of the specimens were 70 and 25 mm, respectively. The clearance (g) between the die and punch was 2.5 mm, and the velocity of the crosshead

of the test machine was set to 0.12 mm/s in all experiments conducted using an MTS test machine, as illustrated in **Fig. 4**. The load-stroke curves were recorded by the machine data acquisition system.

The bend angles at maximum stroke (before springback) were calculated based on the crosshead displacement of 8 mm, which led to the bending angle (θ) of 67.89°, 68.42°, and 69.52° for the sample thickness of 0.1, 0.2 and 0.4 mm, respectively. The bend angles after springback were measured from optical images.

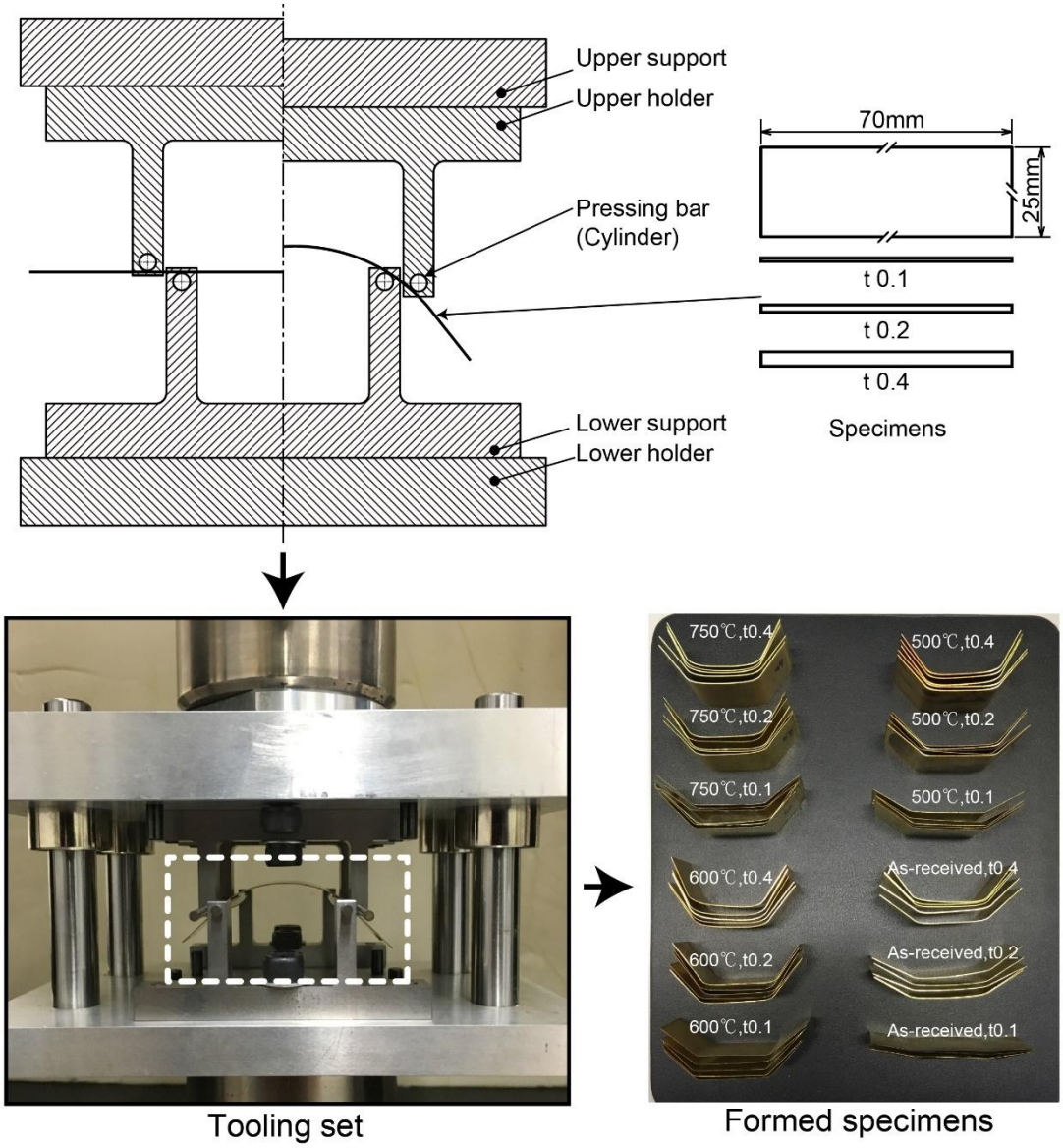

Fig. 4. Tooling configuration and specimens.

2.3.1. Scatter of deformation load

The load-stroke curves are shown in **Fig. 5**. The flow stress increases with decreasing grain size for the same sheet thickness. When the number of grains across the specimen thickness becomes small, deformation load begins to show significant scatter, as a manifestation of the deformation becoming inhomogeneous due to the random distribution of grains. It can be seen from **Fig. 5** (c) that the scatter almost disappears and the deformation load becomes more repeatable for sheet metal samples of larger thickness.

This can be explained by the different scaled deformation behavior. For the sheet metal with the thickness of 0.4 mm, which is considered as a polycrystal material, the deformation behavior is regarded as the macro-scaled uniform deformation and the difference of each single grain is negligible. But in the micro-scaled deformation of the sheet metal with the thickness of 0.1mm, the grains are less and each single grain is deformed randomly along the possible slip orientation, which result in Scatter of deformation load.

2.3.2. Experimental determination of the springback angle

It can be seen from **Fig. 6** that the thickness of sheet metal has a dominant effect on springback angle. The springback angle generally decreases with the increase of sheet thickness regardless of grain size. This is in agreement with the well established fact for macroscopic scale bending deformation. In addition, **Fig. 6** also shows that the springback angle decreases with the increase of the average grain size for the metal sheet samples with the for thickness. With the increase of thickness, the effect of grain size gradually decreases. For the case with the thickness of 0.4 mm, the scatter of the springback angle tends to become small.

In addition to the effects of grain and geometrical sizes, the strain gradient involved in bending process also has an effect on springback angle. To explore the interaction between the geometry and grain size, on the one hand, and strain gradient size effect, on the other, a constitutive model is proposed that takes into consideration both geometry and grain size effect, and the strain gradient size effect.

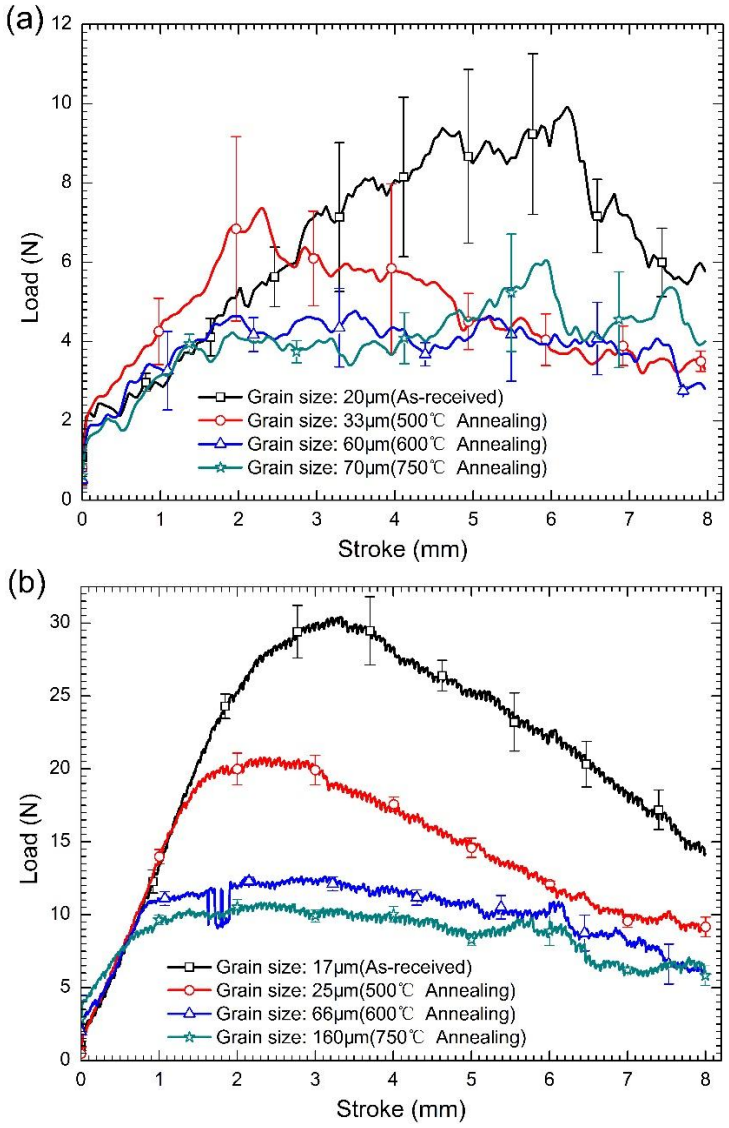

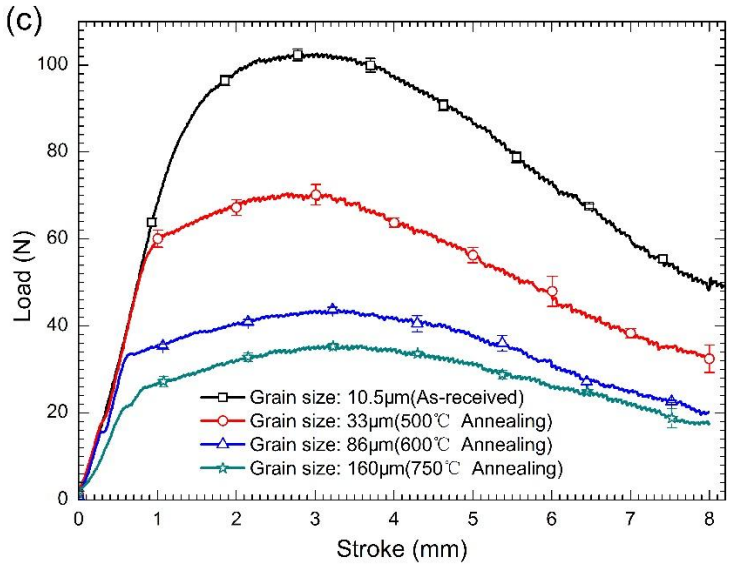

Fig. 5. Load-stroke curve of sheet samples with thickness (a) t=0.1, (b) t=0.2, (c) t=0.4 mm.

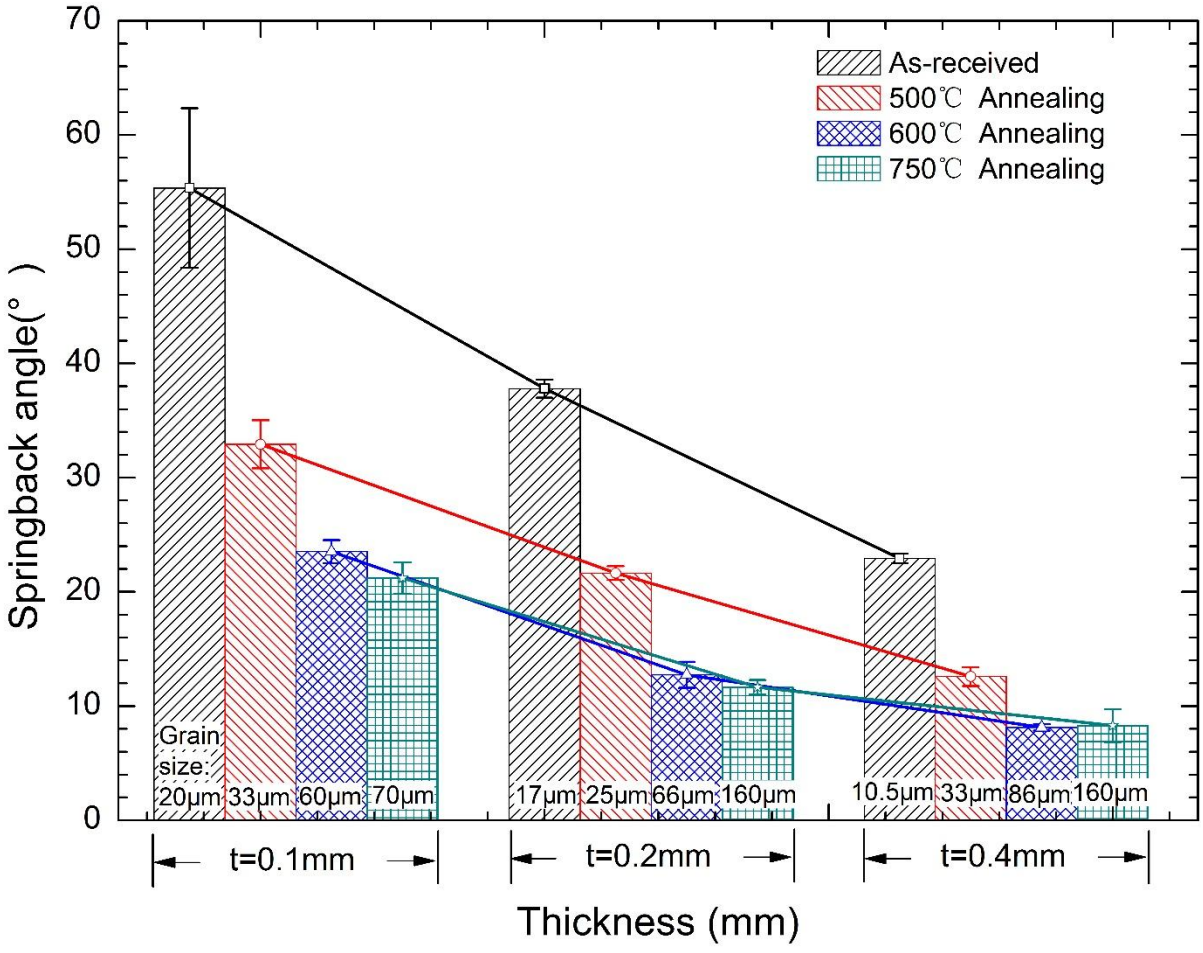

Fig. 6. Experimentally determined springback angles in sheet metal samples with different thickness and grain size.

3. A combined constitutive model incorporating microstructure and strain gradient effects

3.1. Size effect constitutive model

To describe the micro-scale flow stress of sheet metal, the surface layer model (Engel and Eckstein, 2002) was employed. Based on the model, the polycrystalline material is considered to be comprised of surface and inner portions, as shown in **Fig. 7**. Consequently, the flow stress of the material is determined by the contribution from two kinds of flow stresses: the flow stress of inner grains and that of surface grains. Since surface grains experience less constraint than the inner grains, they may undergo easy sliding and rotation, leading to lower flow stress compared to the inner grains. According to this rationale, the overall flow stress of the deforming body can be expressed as follows:

$$\begin{cases} \sigma = \eta\sigma_s + (1-\eta)\sigma_i \\ \eta = \dfrac{N_s}{N} \end{cases} \tag{1}$$

In Eq. (1), σ and N are the flow stress and the total grain number of the material, and σ_s and N_s are the flow stress and the number of surface grains, while σ_i is the flow stress of the inner grains, and η denotes the ratio between the number of surface grains to the number of the grains in the whole deformation body. In macro-forming, the ratio η of the surface grains is negligibly small, so that the contribution from the flow stress of surface grains to the deformation can be ignored. However, when the sample is scaled down to meso- or micro-scale, η increases, and the surface grains play an increasingly important role in the overall deformation response.

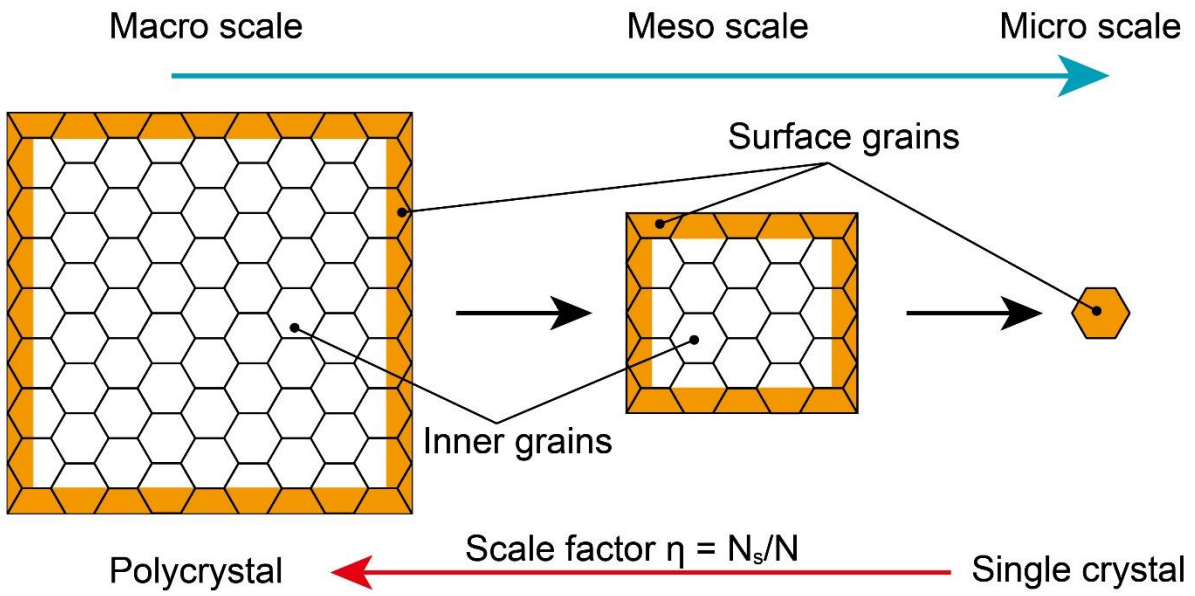

Fig. 7. Schematic identification of the surface and inner grains in a workpiece as a function of overall scale (Peng et al., 2009).

Based on the surface layer model, Lai et al. (Lai et al., 2008) proposed a hybrid constitutive model to describe the flow stress-strain relationship of materials taking into account the size effect. In this model, the surface grains are considered to have properties similar to that of a single crystal, while the inner grains are treated as a polycrystal. In accordance with the crystal plasticity theory and the Hall-Petch equation (Armstrong, 1982; Armstrong et al., 1962), the stresses in the surface and inner grains can be described as follows:

$$\sigma_s(\varepsilon) = m\tau_0(\varepsilon) \tag{2}$$

$$\sigma_i(\varepsilon) = M\left(\tau_0(\varepsilon) + k(\varepsilon)d^{-\frac{1}{2}}\right) \tag{3}$$

In Eqs. (2) and (3), d is the grain size; m and M are the orientation factors of single crystal and polycrystal respectively; $\tau_0(\varepsilon)$ is the critical resolved shear stress of a single crystal, and $k(\varepsilon)$ is the local stress needed for general yield associated with the transmission of

slip across polycrystal grain boundaries (Xu et al., 2015).

Based on the crystal plasticity theory (Argon, 2008), shear stress $\tau_R(\varepsilon)$ can be represented by the lattice friction stress $\tau_0(\varepsilon)$ and the dislocation-induced hardening, expressed in the following form:

$$\tau_R(\varepsilon) = \tau_0(\varepsilon) + \alpha G b\sqrt{\rho_T} = \tau_0(\varepsilon) + \alpha G b\sqrt{\rho_s + \rho_G} \tag{4}$$

where α is an empirical material constant ranging between 0.1 and 0.5, G is shear modulus, b is the Burgers vector magnitude, ρ_T, ρ_s and ρ_G are the total dislocation density, statistically stored dislocation density, and geometrically necessary dislocation density, respectively.

The density of statistically stored dislocations and geometrically necessary dislocations are considered to be monotonic functions of strain represented as:

$$\rho_s(\varepsilon) = \frac{C_s\varepsilon}{bL^s} \tag{5}$$

$$\rho_G(\varepsilon) = \frac{C_G\varepsilon}{bd} \tag{6}$$

where C_S and C_G are material constants, ε, b and L^s are the strain, Burgers vector magnitude and slip length, respectively (Hansen, 1985). Therefore, the total dislocation density takes the following form:

$$\rho_T = \rho_s + \rho_G = \frac{C_S \varepsilon}{bL^s} + \frac{C_G \varepsilon}{bd} \tag{7}$$

In the classical plasticity, only the statistically stored dislocation density $\rho_s(\varepsilon)$ is considered. However, due the significant deformation gradients that exist between sample surface and bulk, geometrically necessary dislocations described by density $\rho_G(\varepsilon)$ may dominate in micro-scaled plastic deformation, whilst the influence of statistically stored dislocations can be neglected, i.e. $\rho_s(\varepsilon) \approx 0$. Based on Swift's hardening model, $\tau(\varepsilon) = k(\varepsilon)^n$, the constitutive model for macro-scale deformation is proposed as:

$$\sigma_i(\varepsilon) = M\left(\tau_0(\varepsilon) + \alpha Gb\sqrt{\rho_T}\right) = M\left(\tau_0(\varepsilon) + \alpha Gb\sqrt{\frac{C_G\varepsilon}{bd}}\right) = Mk(\varepsilon)^n + M\alpha Gb\sqrt{\frac{C_G\varepsilon}{bd}} \tag{8}$$

Combining Eqs. (1) and (8), the flow stress of material in meso/micro-scale deformation can be formulated as:

$$\sigma(\varepsilon) = \eta m k_1(\varepsilon)^{n_1} + (1-\eta)\left(Mk_2(\varepsilon)^{n_2} + M\alpha Gb\sqrt{\frac{C_G\varepsilon}{bd}}\right) \tag{9}$$

When the size factor is set to η = 0, the above flow stress expression corresponds to the polycrystal model. When the size factor is set to η = 1, the flow stress expression corresponds to the single crystal model.

The schematic cross section of the sheet at the micro-scale is shown in **Fig.8**. The grain diameter of sheet material is denoted by *d*. The sheet thickness and width are denoted by *t*

and w, respectively. In micro forming, w is usually much larger than t and d. Hence, according to Eq. (1), the ratio of the surface grains in the section can be simplified to:

$$\eta = \frac{N_s}{N} = \frac{2(wd/2)/d^2}{wt/d^2} = \frac{d}{t} \tag{10}$$

By using the curve fitting approach, the constants k_1, k_2, n_1 and n_2 can be determined, and $k_1 = k_2 = 274$, $n_1 = n_2 = 0.48$, C_G= *0.18*, α= *0.34* (Rodriguez and Gutierrez, 2003), m and M are set to be 2 and 3.06 (Clausen et al., 1998; Mecking and Kocks, 1981) for all materials. The subscript is used to differentiate the stress in surface grains in Eq. (9).

The comparison between the calculation result and the true stress–strain curve from the actual experiment is shown in **Fig. 3**, the solid lines being true stress–strain curves obtained by curve fitting, and the markers represent experiment results.

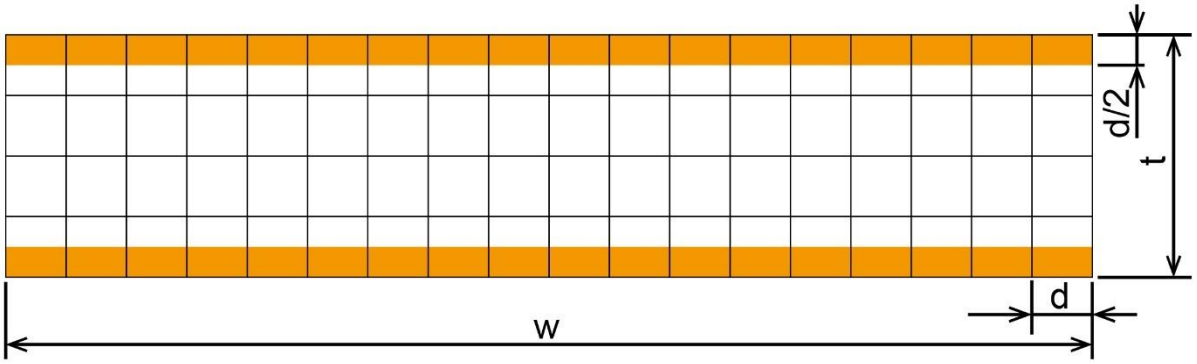

Fig. 8. The surface layer model of the sheet samples at the meso/micro-scale.

3.2. Constitutive model with plastic strain gradient

Taking the plastic strain gradient hardening into account in the constitutive model, the following flow stress model is proposed:

$$\sigma(\varepsilon)=\eta m k_1(\varepsilon)^{n_1}+(1-\eta)\left(Mk_2(\varepsilon)^{n_2}+M\alpha Gb\sqrt{\frac{C_G\varepsilon}{bd}}\right)+k_3 l\left|\nabla\varepsilon\right| \tag{11}$$

where the presence of the term $\left|\nabla\varepsilon\right|$ indicates the contribution of the plastic strain gradient to the flow stress, with l denoting the material intrinsic length, and $k_3=k_1=k_2$.

The variation of the plastic strain gradient in the thickness direction with longitudinal coordinate is given by:

$$\nabla\varepsilon=\frac{\left[\left(R_i+t\right)d\theta-R_n d\theta\right]-\left(R_i d\theta-R_n d\theta\right)}{tR_n d\theta}=\frac{1}{R_n}=c \tag{12}$$

Using conventional effective plastic strain, Eq. (11) could be rewritten as:

$$\overline{\sigma}(\varepsilon)=\eta m k_1\left(\overline{\varepsilon}\right)^{n_1}+(1-\eta)\left(Mk_2\left(\overline{\varepsilon}\right)^{n_2}+M\alpha Gb\sqrt{\frac{C_G\overline{\varepsilon}}{bd}}\right)+k_3 l\left|\nabla\overline{\varepsilon}\right| \tag{13}$$

The material intrinsic length (l) parameter is the multiplier of the strain gradient and determines the characteristic dimension of the size effect encountered in micro- and nano-scale deformation (Abu Al-Rub and Voyiadjis, 2004), and can be calculated based on semi-empirical expression.

Xue et al. (Xue et al., 2002) has proposed the following equation to calculate the intrinsic length l:

$$l=18\alpha^2\left(\frac{G}{\sigma_{s0}}\right)^2 b \tag{14}$$

3.3. The calculation of strain, strain gradient, stress, and bending moment

3.3.1. The calculation of strain and strain gradient

The geometric model of microbending deformation is illustrated in **Fig. 9**. The axes of the local coordinate system $\vec{e_1}$, $\vec{e_2}$ $\vec{e_3}$ are along the width, thickness and length directions, respectively (with the latter direction not shown in the figure). Since the width *w* is much larger than the sheet thickness *t*, plane strain deformation is assumed. The displacement field is supposed as (Stölken and Evans, 1998):

$$\mu_1 = ce_1e_2 , \mu_2 = \frac{-c\left(e_1^{\,2} + e_2^{\,2}\right)}{2} , \mu_3 = 0 \tag{15}$$

So, the strain tensor can be expressed as:

$$\left[\varepsilon_{ij}\right] = \begin{bmatrix} ce_2 & 0 & 0 \\ 0 & -ce_2 & 0 \\ 0 & 0 & 0 \end{bmatrix} \tag{16}$$

The conventional effective strain is:

$$\bar{\varepsilon} = \sqrt{\frac{2}{3}\varepsilon'_{ij}\varepsilon'_{ij}} = \frac{2}{\sqrt{3}}ce_2 \tag{17}$$

The gradient of effective strain is given by:

$$\nabla\bar{\varepsilon} = \begin{bmatrix} 0 & \frac{2}{\sqrt{3}}c & 0 \end{bmatrix} \tag{18}$$

$$\left|\nabla\bar{\varepsilon}\right| = \frac{2}{\sqrt{3}}c \tag{19}$$

When Eqs. (17) and (19) are substituted into Eq.(14), the constitutive relation used in the

analytical model is obtained:

$$\overline{\sigma}(\varepsilon)=\eta m k_1\left(\frac{2}{\sqrt{3}}ce_2\right)^{n_1}+(1-\eta)\left[Mk_2\left(\frac{2}{\sqrt{3}}ce_2\right)^{n_2}+M\alpha Gb\sqrt{\frac{C_1}{bd}}\sqrt{\frac{2}{\sqrt{3}}ce_2}\right]+\frac{2}{\sqrt{3}}k_3lc \qquad (20)$$

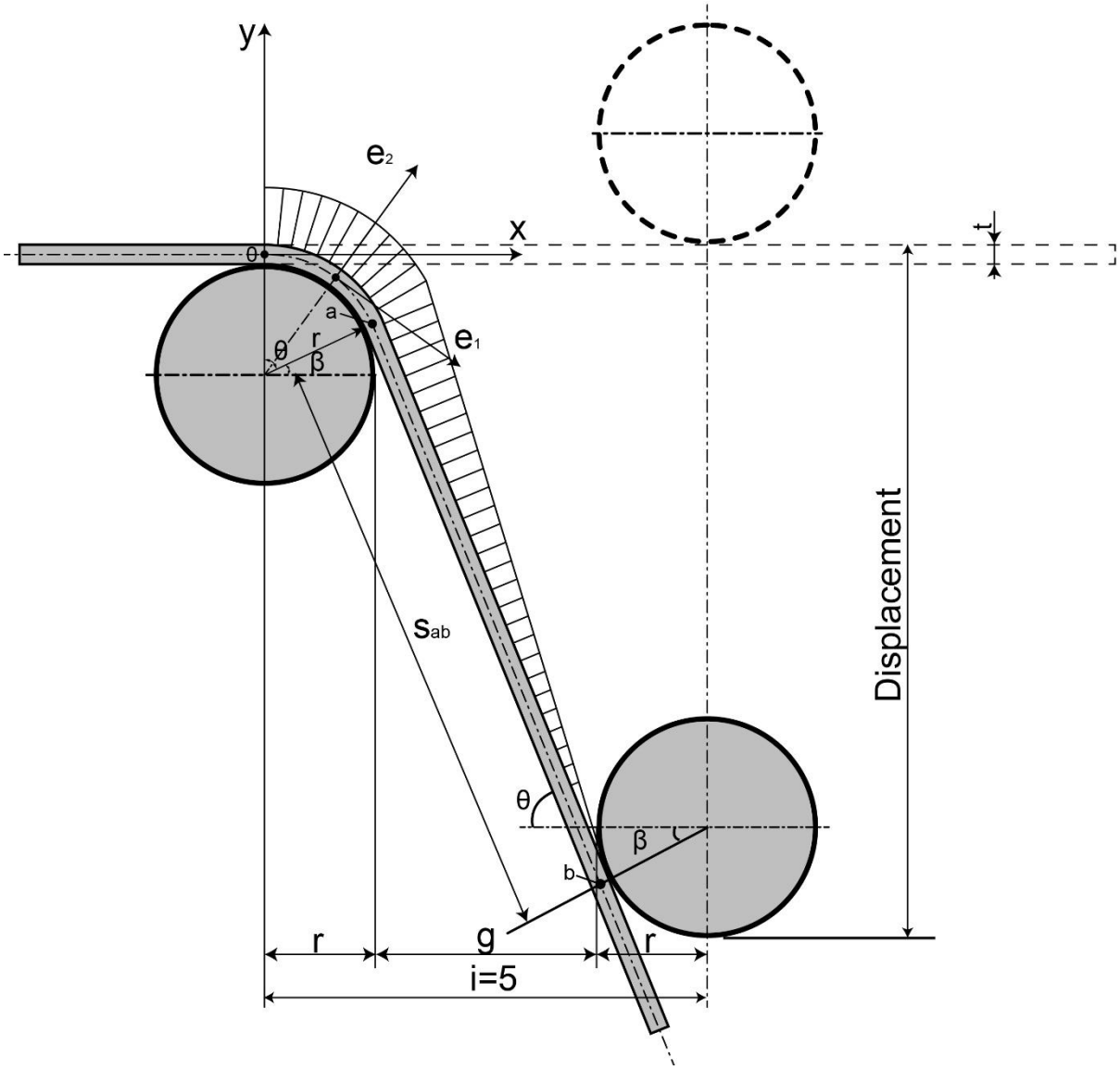

Fig. 9. Geometric schematic diagram of microbending deformation

3.3.2. The calculation of stress

For sheet microbending, the radial stress normal to the sheet is assumed to be vanishingly

small (plane stress state), and only stresses along the longitudinal and width direction are considered,

$$\sigma_2 = 0 \quad , \quad \sigma_3 = \frac{1}{2}\sigma_1 \tag{21}$$

Thus, the effective stress is:

$$\bar{\sigma} = \sqrt{\frac{3}{2}\sigma_{ij}^{'}\sigma_{ij}^{'}} = \frac{\sqrt{3}}{2}\sigma_1 \tag{22}$$

In microbending deformation, a sheet section may deform elastically, or may contain an elastic core. In such elastically deformed region, the stress is:

$$\sigma_1 = \frac{E}{1-\nu^2}\varepsilon_1 \qquad 0 < \bar{\varepsilon} < \varepsilon_E \tag{23}$$

where ε_E is the elastic strain limit.

Substituting Eq. (22) into Eq. (20), the constitutive equation of the plastic deformation region is formulated as:

$$\sigma_1 = \frac{2}{\sqrt{3}}\left\{\eta m k_1 \left(\frac{2}{\sqrt{3}}ce_2\right)^{n_1} + (1-\eta)\left[Mk_2\left(\frac{2}{\sqrt{3}}ce_2\right)^{n_2} + M\alpha Gb\sqrt{\frac{C_G}{bd}}\sqrt{\frac{2}{\sqrt{3}}ce_2}\right] + \frac{2}{\sqrt{3}}k_3 lc\right\} \tag{24}$$

3.3.3. The calculation of bending moment

The bending moment is calculated as:

$$M = \int_0^t \sigma_1 e_2 w \cdot de_2 \tag{25}$$

For the stress within the elastic region, as shown in **Fig. 10**, the elastic bending moment can

be expressed based on Eqs. (23) and (25) as follows:

$$M_E = \int_{-e_{2E}}^{e_{2E}} \sigma_1 e_2 w \cdot de_2 = \frac{2wE}{3(1-\nu^2)} c\left(e_{2E}\right)^3 \tag{26}$$

As for the plastic deformation region illustrated **Fig. 10**, the plastic bending moment can be obtained based using Eqs. (24) and (25):

$$\begin{aligned} M_P &= 2\int_{e_{2E}}^{t/2} \sigma_1 e_2 w \cdot de_2 \\ &= \frac{4w}{\sqrt{3}} \int_{e_{2E}}^{t/2} \left\{ \eta m k_1 \left(\frac{2}{\sqrt{3}} c e_2 \right)^{n_1} + (1-\eta) \left[M k_2 \left(\frac{2}{\sqrt{3}} c e_2 \right)^{n_2} + M \alpha G b \sqrt{\frac{C_G}{bd}} \sqrt{\frac{2}{\sqrt{3}} c e_2} \right] + \frac{2}{\sqrt{3}} k_3 l c \right\} e_2 \cdot de_2 \\ &= \frac{4w}{\sqrt{3}} \left\{ \begin{array}{l} \dfrac{\eta m k_1 \left(2/\sqrt{3}\, c\right)^{n_1}}{n_1+2} \left[\left(\frac{t}{2}\right)^{n_1+2} - {e_{2E}}^{n_1+2} \right] + \dfrac{(1-\eta) M k_2 \left(2/\sqrt{3}\, c\right)^{n_2}}{n_2+2} \left[\left(\frac{t}{2}\right)^{n_2+2} - {e_{2E}}^{n_2+2} \right] \\ + (1-\eta) M \alpha G b \sqrt{\dfrac{C_G}{bd}} \sqrt{\dfrac{2}{\sqrt{3}} c} \dfrac{2}{5} \left[\left(\frac{t}{2}\right)^{5/2} - {e_{2E}}^{5/2} \right] + \dfrac{1}{\sqrt{3}} k_3 l c \left[\left(\frac{t}{2}\right)^{2} - {e_{2E}}^{2} \right] \end{array} \right\} \end{aligned} \tag{27}$$

For completely plastic bending i.e. ($e_{2E} = 0$), the plastic bending moment is represented by:

$$M_P = \frac{4w}{\sqrt{3}} \left\{ \begin{array}{l} \dfrac{\eta m k_1 \left(2/\sqrt{3}\, c\right)^{n_1}}{n_1+2} \left(\frac{t}{2}\right)^{n_1+2} + \dfrac{(1-\eta) M k_2 \left(2/\sqrt{3}\, c\right)^{n_2}}{n_2+2} \left(\frac{t}{2}\right)^{n_2+2} \\ + (1-\eta) M \alpha G b \sqrt{\dfrac{C_G}{bd}} \sqrt{\dfrac{2}{\sqrt{3}} c} \dfrac{2}{5} \left(\frac{t}{2}\right)^{5/2} + \dfrac{1}{\sqrt{3}} k_3 l c \left(\frac{t}{2}\right)^{2} \end{array} \right\} \tag{28}$$

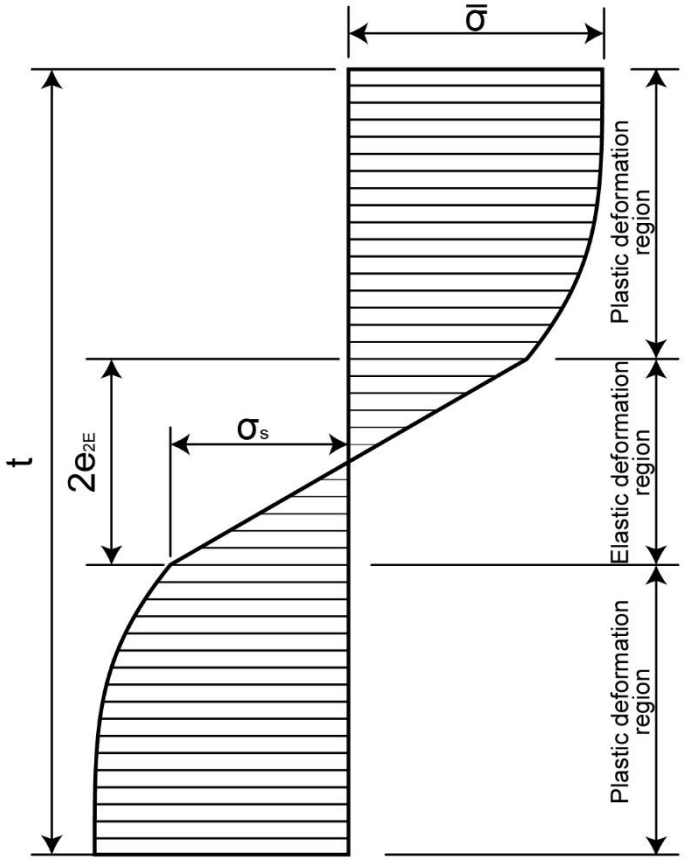

Fig. 10. Stress distribution along sheet thickness direction.

3.4. Calculation of springback angle

After microbending, if the neutral radius of the bent sheet changes from R_n to $R_n^{'}$, the curvature change before and after bending is:

$$\Delta c = \frac{1}{R_n} - \frac{1}{R_n^{'}} = \frac{M_b}{I} \cdot \frac{1-\nu^2}{E} \tag{29}$$

where, M_b is the bending moment at a section of the sheet; $I = wt^3/12$ is the second moment of area.

The springback angle of an infinitesimal segment of the bent sheet is obtained as:

$$d\theta_s = \Delta c \cdot ds = \frac{M_b}{I} \cdot \frac{1-\nu^2}{E} \cdot ds \tag{30}$$

where ds is the segment length. The total springback angle of the bent sheet can be calculated by integrating Eq. (30) across the total bending range:

$$\theta_s = \int_0^b \frac{M_b}{I} \cdot \frac{1-\nu^2}{E} \cdot ds = \int_0^a \frac{M_p}{I} \cdot \frac{1-\nu^2}{E} \cdot ds + \int_a^b \frac{M_p}{I} \cdot \frac{1-\nu^2}{E} \cdot \frac{s}{s_a} \cdot ds = \frac{M_p}{I} \cdot \frac{1-\nu^2}{E} \left(\widehat{s}_{oa} + s_{ab} \right) \tag{31}$$

where $\widehat{s}_{oa}$ is the die-sheet contact arc length.

$$\widehat{s}_{oa} = \left(r + \frac{t}{2} \right) \cdot \theta \tag{32}$$

Referring to the geometric relation shown in **Fig. 9**, the length s_{ab} from point *b* to *a* can be calculated as:

$$s_{ab} = \left[i - 2\left(r + \frac{t}{2} \right) \sin\theta \right] \Big/ \cos\theta \tag{33}$$

where θ is the bending angle, and $i=g+2r$.

4. Results and discussion

4.1. Prediction of the springback angle

According to Eq. (30), the analytical calculation of springback angle can be obtained and the prime influence factors also can be determined, which include material Young's modulus (E), geometrical parameters of sheet metal and tooling, such as sheet metal thickness (t), cylinder radius (r), clearance (g), and plastic bending moment M_p. The springback angle after U-microbending is calculated with the analytical model and compared with the experimental

data with the different sheet thickness of 0.1, 0.2, and 0.4 mm for the constant bending angle, as shown in **Fig. 11**.

The data illustrates that the springback angle predicted by the analytical equation based on the mixed constitutive model is close to the experimental data, which means the proposed mixed model does capture the geometric size effect and strain gradient effect.

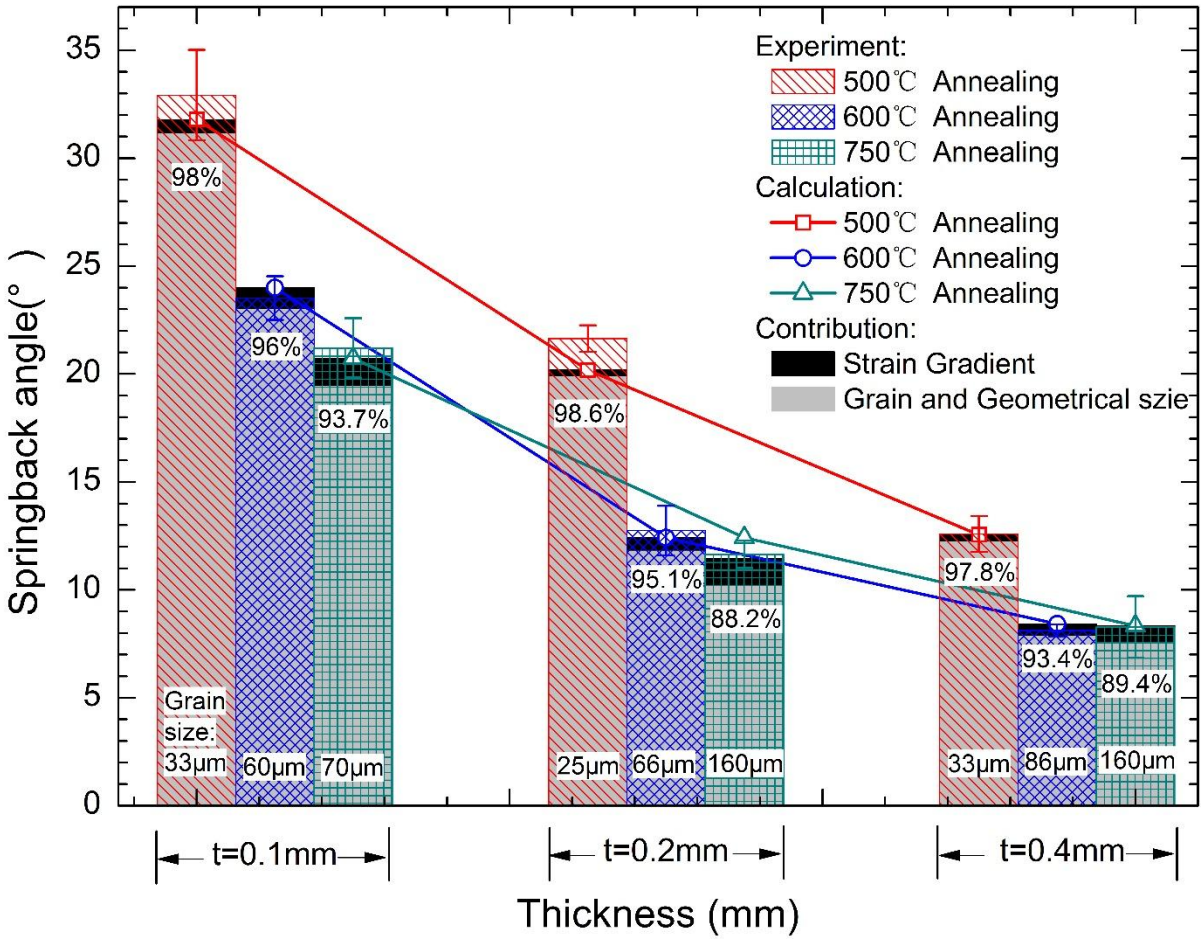

Fig. 11. Comparison of the springback angles between experiment and calculation for sheet metal samples with different thickness and grain sizes.

4.2. Contribution to springback

The mixed constitutive model takes into account the size effect and strain gradient simultaneously. On the other hand, the contribution to springback can be determined by employing constitutive models that only consider the geometric size effect and the strain gradient effect separately. The contribution expressed as percentage of the overall effect is shown in **Fig. 11**. The contribution of the geometric size effect to springback is greater than 90% for almost all cases. It can be concluded that geometric size effect exerts a dominant influence on springback in comparison with the strain gradient for sheet samples with the thickness of 0.1, 0.2, and 0.4mm, respectively.

The contribution to springback from the strain gradient effect varies with the sheet thickness and grain size. According to the proposed constitutive model, the strain gradient contribution can be evaluated quantitatively, and plot the result as shown in **Fig. 12**. It is apparent that the contribution to springback from the strain gradient effect decreases with the increase of sheet thickness, and with the decrease of grain size. As the sheet thickness increases, the plastic strain gradient hardening effect becomes weaker. For the cases of sheet thickness greater than 0.2 mm and annealed at 500 ^{o}C and 600 ^{o}C, the plastic strain gradient does not change significantly. For the case with fewer grains in the through-thickness direction, the plastic strain gradient plays a greater role than the case with relatively greater number grains, which reflects the fact that deformed coarse-grained sheet have a greater geometrically necessary dislocation density.

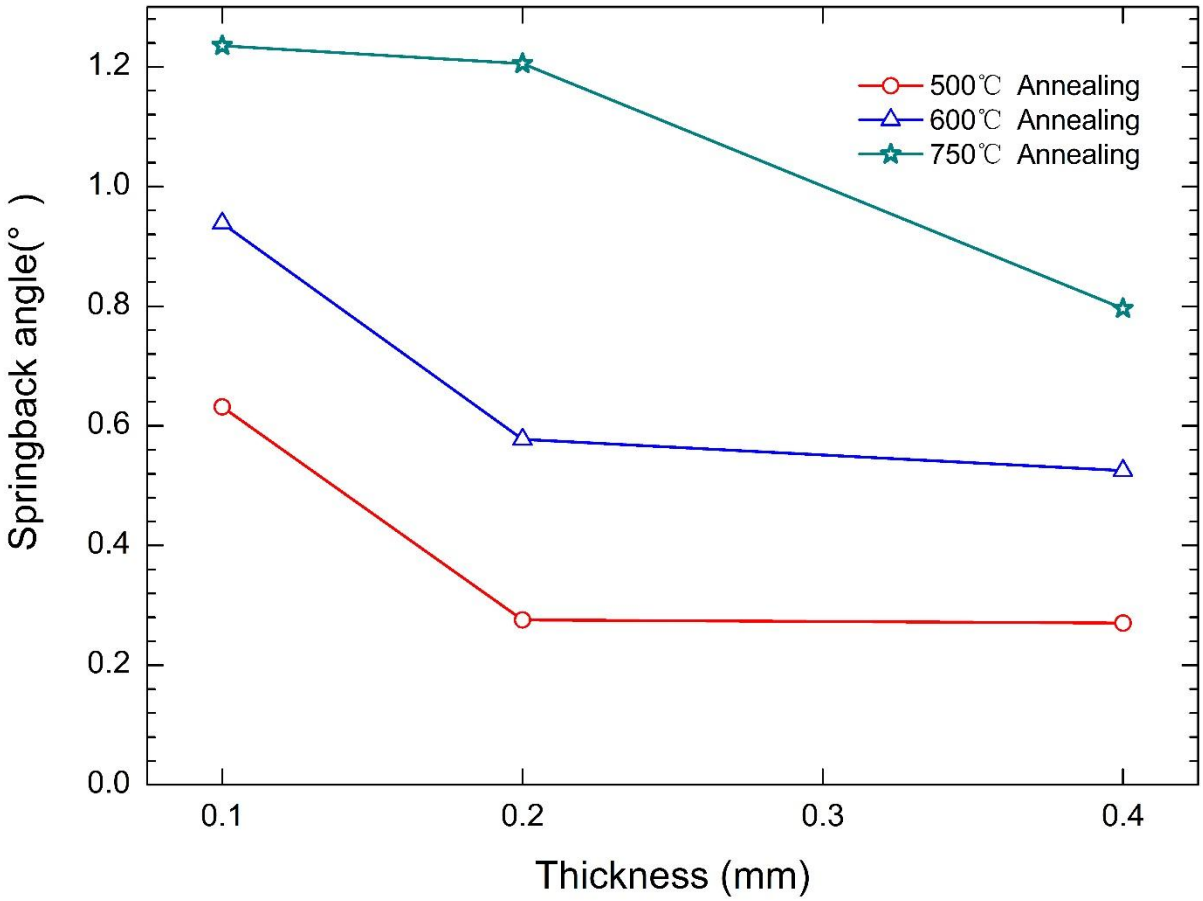

Fig. 12. The contribution of strain gradient to springback for sheet metal samples with different thicknesses and grain sizes.

5. Conclusions

Springback behaviour of sheet metal in micro-bending process is not only affected by size effect, but also by strain gradient effect. In order to investigate the interaction between these two effects, a free U-microbending experiment was conducted using the copper alloy sheet with different thickness of 0.1, 0.2, and 0.4mm. The experiment results showed that the thickness of sheet metal has a dominant effect on springback and the springback decreases with the increase of sheet thickness regardless of grain size. A mixed constitutive model was then proposed based on the surface layer model and strain gradient. The proposed model was used to predict the springback in micro-scale bending process. The following conclusions are drawn from this research:

1. The combined constitutive model which simultaneously considers the size effect and the strain gradient effect was firstly proposed. The calculated springback angle on the basis of the model has a good agreement with the experimental results.
2. The size effect has an absolutely dominant influence on springback in comparison with the strain gradient for the sheet with the thickness of 0.1, 0.2, and 0.4 mm. The contribution of size effect to springback is about 90% more for almost all the cases.
3. The quantitative expression of contribution of each effect on springback can be obtained based on the proposed mixed constitutive model. The contribution to springback from the strain gradient decreases with increase of sheet thicknesses and the decrease of grain sizes.

Acknowledgement

The authors would like to the funding support to this research from the project BQ33F of the General Research Fund, the projects of G-UA8U, G-YBDM and G-YBL2 from The Hong Kong Polytechnic University, and the project of No. 51575465 from the National Natural Science Foundation of China.

References

Abu Al-Rub, R.K., Voyiadjis, G.Z., 2004. Analytical and experimental determination of the material intrinsic length scale of strain gradient plasticity theory from micro- and nano-indentation experiments. Int. J. Plast. 20, 1139-1182.

Argon, A.S., 2008. Strengthening mechanisms in crystal plasticity. Oxford University Press Oxford.

Armstrong, R., 1982. The yield and flow stress dependence on polycrystal grain size. Yield, flow and fracture of polycrystals, 1-31.

Armstrong, R., Codd, I., Douthwaite, R., Petch, N., 1962. The plastic deformation of polycrystalline aggregates. Philos Mag 7, 45-58.

Clausen, B., Lorentzen, T., Leffers, T., 1998. Self-consistent modelling of the plastic deformation of fcc polycrystals and its implications for diffraction measurements of internal stresses. Acta Mater. 46, 3087-3098.

Diehl, A., Engel, U., Geiger, M., 2008. Mechanical properties and bending behaviour of metal foils. Proceedings of the Institution of Mechanical Engineers. Part B. Journal of engineering manufacture 222, 83-91.

Diehl, A., Engel, U., Geiger, M., 2010. Influence of microstructure on the mechanical properties and the forming behaviour of very thin metal foils. Int J Adv Manuf Tech 47, 53-61.

Engel, U., Eckstein, R., 2002. Microforming - from basic research to its realization. J. Mater. Process. Technol. 125, 35-44.

Fleck, N., Hutchinson, J., 1993. A phenomenological theory for strain gradient effects in

plasticity. Journal of the Mechanics and Physics of Solids 41, 1825-1857.

Fleck, N., Hutchinson, J., 2001. A reformulation of strain gradient plasticity. Journal of the Mechanics and Physics of Solids 49, 2245-2271.

Fu, M., Wang, J., Korsunsky, A., 2016. A review of geometrical and microstructural size effects in micro-scale deformation processing of metallic alloy components. International Journal of Machine Tools and Manufacture 109, 94-125.

Fu, M.W., Chan, W.L., 2013. A review on the state-of-the-art microforming technologies. Int J Adv Manuf Tech 67, 2411-2437.

Geiger, M., Kleiner, M., Eckstein, R., Tiesler, N., Engel, U., 2001. Microforming. CIRP Annals - Manufacturing Technology 50, 445-462.

Hall, E.O., 1951. The Deformation and Ageing of Mild Steel: III Discussion of Results. Proceedings of the Physical Society. Section B 64, 747.

Hansen, N., 1985. Polycrystalline strengthening. Metall. Trans. A 16, 2167-2190.

Lai, X., Peng, L., Hu, P., Lan, S., Ni, J., 2008. Material behavior modelling in micro/meso-scale forming process with considering size/scale effects. Comput. Mater. Sci. 43, 1003-1009.

Li, H., Dong, X., Shen, Y., Diehl, A., Hagenah, H., Engel, U., Merklein, M., 2010. Size effect on springback behavior due to plastic strain gradient hardening in microbending process of pure aluminum foils. Mater. Sci. Eng., A 527, 4497-4504.

Liu, J.G., Fu, M.W., Lu, J., Chan, W.L., 2011. Influence of size effect on the springback of sheet metal foils in micro-bending. Comput. Mater. Sci. 50, 2604-2614.

Mecking, H., Kocks, U., 1981. Kinetics of flow and strain-hardening. Acta Metall. 29,

1865-1875.

Meyers, M.A., Ashworth, E., 1982. A Model for the Effect of Grain-Size on the Yield Stress of Metals. Philos. Mag. A 46, 737-759.

Nix, W.D., Gao, H., 1998. Indentation size effects in crystalline materials: a law for strain gradient plasticity. Journal of the Mechanics and Physics of Solids 46, 411-425.

Peng, L., Lai, X., Lee, H.-J., Song, J.-H., Ni, J., 2009. Analysis of micro/mesoscale sheet forming process with uniform size dependent material constitutive model. Mater. Sci. Eng., A 526, 93-99.

Petch, N.J., 1953. The Cleavage Strength of Polycrystals. J. Iron Steel Inst. 174, 25-28.

Ran, J.Q., Fu, M.W., 2014. A hybrid model for analysis of ductile fracture in micro-scaled plastic deformation of multiphase alloys. Int. J. Plast. 61, 1-16.

Ran, J.Q., Fu, M.W., Chan, W.L., 2013. The influence of size effect on the ductile fracture in micro-scaled plastic deformation. Int. J. Plast. 41, 65-81.

Rodriguez, R., Gutierrez, I., 2003. Correlation between nanoindentation and tensile properties: Influence of the indentation size effect. Mater. Sci. Eng., A 361, 377-384.

Stölken, J.S., Evans, A.G., 1998. A microbend test method for measuring the plasticity length scale. Acta Mater. 46, 5109-5115.

Vollertsen, F., Niehoff, H.S., Hu, Z., 2006. State of the art in micro forming. International Journal of Machine Tools and Manufacture 46, 1172-1179.

Wagoner, R.H., Lim, H., Lee, M.-G., 2013. Advanced Issues in springback. Int. J. Plast. 45, 3-20.

Wang, J.L., Fu, M.W., Ran, J.Q., 2014. Analysis of the Size Effect on Springback Behavior in

Micro-Scaled U-Bending Process of Sheet Metals. Adv. Eng. Mater. 16, 421-432.

Wang, S., Zhuang, W., Balint, D., Lin, J., 2009. A virtual crystal plasticity simulation tool for micro-forming. Procedia Engineering 1, 75-78.

Wang, W., Huang, Y., Hsia, K.J., Hu, K.X., Chandra, A., 2003. A study of microbend test by strain gradient plasticity. Int. J. Plast. 19, 365-382.

Xu, Z.T., Peng, L.F., Fu, M.W., Lai, X.M., 2015. Size effect affected formability of sheet metals in micro/meso scale plastic deformation: Experiment and modeling. Int. J. Plast. 68, 34-54.

Xue, Z., Huang, Y., Li, M., 2002. Particle size effect in metallic materials: a study by the theory of mechanism-based strain gradient plasticity. Acta Mater. 50, 149-160.

Zbib, H., Aifantis, E., 2003. Size effects and length scales in gradient plasticity and dislocation dynamics. Scripta Mater. 48, 155-160.

Zhu, H.X., Karihaloo, B.L., 2008. Size-dependent bending of thin metallic films. Int. J. Plast. 24, 991-1007.

Zhuang, W., Lin, J., 2008. An integrated micromechanics modelling approach for micro-forming simulation. Int. J. Mod Phys B 22, 5907-5912.

Zhuang, W., Wang, S., Cao, J., Lin, J., Hartl, C., 2010. Modelling of localised thinning features in the hydroforming of micro-tubes using the crystal-plasticity FE method. Int. J. Adv. Manuf. Technol. 47, 859-865.